Seven-Coordinated Pnicogens. Synthesis and Characterization of the SbF_7^{2-} and BiF_7^{2-} Dianions and a Theoretical Study of the AsF_7^{2-} Dianion

Greg W. Drake,*,† David A. Dixon,‡ Jeffrey A. Sheehy,† Jerry A. Boatz,† and Karl O. Christe*,§,||

Contribution from Raytheon STX and the Propulsion Directorate, Air Force Research Laboratory, Edwards Air Force Base, California 93524, Loker Hydrocarbon Research Institute, University of Southern California, Los Angeles, California 90089, and Pacific Northwest National Laboratory, Richland, Washington 99352

Received February 19, 1998

Abstract: The novel seven-coordinated BiF_7^{2-} and SbF_7^{2-} dianions have been prepared and characterized. The Cs_2BiF_7, Rb_2BiF_7, K_2BiF_7, and Na_2BiF_7 salts were obtained in high yield by heating BiF_5 with an excess of the corresponding alkali metal fluorides to about 250 °C. Attempts failed to prepare the corresponding BiF_8^{3-} salts or Li_2BiF_7 under similar conditions. The $[N(CH_3)_4]_2BiF_7$ salt was obtained by the combination of excess $N(CH_3)_4F$ with BiF_5 in CH_3CN solution at −31 °C. The $(NO_2)_2BiF_7$ salt was prepared from BiF_5 and a large excess of liquid FNO at −78 °C and decomposes at room temperature to $NOBiF_6$ and FNO. The corresponding Cs_2SbF_7, K_2SbF_7, and $[N(CH_3)_4]_2SbF_7$ salts were also synthesized in a similar fashion, but Na_2SbF_7 was not formed. The pronounced fluoride ion affinity of SbF_6^- was further demonstrated by the formation of some Cs_2SbF_7 when dry CsF and $CsSbF_6$ were ball-milled at room temperature. The BiF_7^{2-} and SbF_7^{2-} anions, which are the first examples of binary pnicogen compounds with coordination numbers in excess of six, were characterized by vibrational spectroscopy and ab initio electronic structure calculations. They possess pentagonal bipyramidal, highly fluxional structures of D_{5h} symmetry, similar to those of IF_7 and TeF_7^-, which are isoelectronic with SbF_7^{2-}. Although our theoretical calculations indicate that AsF_7^{2-} is also vibrationally stable, experiments to prepare this dianion were unsuccessful.

Introduction

Except for cluster compounds, such as $[Rh_{10}As(CO)_{22}]^{3-}$ and $[Rh_{12}Sb(CO)_{27}]^{3-}$, in which the pnicogen atoms are located inside a cluster cavity,[1,2] the maximum coordination numbers (CN) reported for binary antimony and bismuth compounds, as a rule, do not exceed six. Even in the triply charged $SbCl_6^{3-}$, $SbBr_6^{3-}$, and $BiCl_6^{3-}$ anions, in which the central atom possesses, in addition to the six halogen ligands, a free valence electron pair, the latter is sterically inactive, and CN 6 is not exceeded.[3−5] CN 6 had been generally accepted as the coordination limit for the pnicogens, and it appears that, probably due to the "magic" stability traditionally attributed to the sp^3 and sp^3d^2 valence electron shells, no systematic efforts have been made to expand the 12 valence electron shells in the hexafluoropnictate(V) anions. However, the relatively high F^- ion affinity of TeF_6 (∼80 kcal mol^{-1})[6] and its ability to bind not only one but also two F^- ions with formation of the TeF_7^- and TeF_8^{2-} anions, respectively,[7−10] suggested that isoelectronic SbF_6^- might also possess sufficient Lewis acidity to add a second F^- ion and form a stable SbF_7^{2-} dianion. Therefore, it was interesting to explore whether the well-known heavier hexafluoropnictate anions, AsF_6^-,[11,12] SbF_6^-,[12,13] and BiF_6^-,[14] could bind additional F^- ligands and form multiply charged anions with coordination numbers higher than six.

Experimental Section

Materials and Methods. The synthesis of anhydrous $N(CH_3)_4F$ has been previously described.[15] The alkali metal fluorides were fused in platinum crucibles, transferred while hot to the drybox, and finely powdered. Antimony pentafluoride and AsF_5 (Ozark Mahoning Co.) were purified by fractional condensation. Bismuth pentafluoride (Ozark Mahoning Co.) did not contain any detectable impurities and was used as received. Acetonitrile (Baker, bioanalyzed, with a water content of less than 40 ppm) was treated with P_2O_5 and freshly distilled prior to

† Propulsion Directorate, Air Force Research Laboratory.
‡ Pacific Northwest National Laboratory.
§ Raytheon STX.
|| University of Southern California.

(1) Vidal, J. L. *Inorg. Chem.* **1981**, *20*, 243.
(2) Vidal, J. L.; Troup, J. M. *J. Organomet. Chem.* **1981**, *213*, 351.
(3) Gillespie, R. J.; Hargittai, I. *The VESPR Model of Molecular Geometry*; Allyn and Bacon: Boston, 1991.
(4) Klapötke, T. M.; Torrieporth-Oetting, I. C. *Nichtmetallchemie*; VSH: Weinheim, Germany, 1994.
(5) Greenwood, N. N.; Earnshaw, A. *Chemistry of the Elements*; Pergamon Press: Oxford, 1984.
(6) Dixon, D. A.; Christe, K. O. Unpublished results based on ab initio calculations.
(7) Muetterties, E. L. *J. Am. Chem. Soc.* **1957**, *79*, 1004.
(8) Selig, H.; Sarig, S.; Abramowitz, S. *Inorg. Chem.* **1974**, *13*, 1508.
(9) Christe, K. O.; Sanders, J. C. P.; Schrobilgen, G.; Wilson, W. W. *J. Chem. Soc., Chem. Commun.* **1991**, 837.
(10) Zhang, X.; Seppelt, K. *Z. Anorg. Allg. Chem.* **1997**, *623*, 491.
(11) Weidlein, J.; Dehnicke, K. *Z. Anorg. Allg. Chem.* **1965**, *337*, 113.
(12) Christe, K. O.; Maya, W. *Inorg. Chem.* **1969**, *8*, 1253.
(13) Begun, G. M.; Rutenberg, A. C. *Inorg. Chem.* **1967**, *6*, 2212.
(14) Christe, K. O.; Wilson, W. W.; Schack, C. J. *J. Fluorine Chem.* **1978**, *11*, 71. Christe K. O.; Wilson, W. W.; Schack, C. J.; Bougon, R. *J. Fluorine Chem.* **1978**, *12*, 336.
(15) Christe, K. O.; Wilson, W. W.; Wilson, R. D.; Bau, R.; Feng, J. *J. Am. Chem. Soc.* **1990**, *112*, 7619.

S0002-7863(98)00572-1 CCC: $15.00
Published on Web 08/08/1998

use. The F_2 (Air Products) was passed through a NaF scrubber for the removal of HF. Nitrosyl fluoride was prepared from NO and F_2 at −196 °C in a Teflon−FEP U-trap and purified by fractional condensation.[16]

Acetonitrile was transferred in a flamed-out Pyrex glass vacuum line that was equipped with Kontex glass−Teflon valves and a Heise pressure gauge. The oxidizers were handled in a stainless steel vacuum line equipped with Teflon−FEP U-traps, 316 stainless steel bellows seal valves, and a Heise pressure gauge.[17] Solids were handled in the dry nitrogen atomosphere of a glovebox.

Infrared spectra were recorded on either a Perkin-Elmer model 283 or a Mattson Galaxy spectrometer using AgBr disks prepared by pressing the finely powdered sample between two thin AgBr plates in a Barnes Engineering minipress inside the glovebox. Raman spectra were recorded on either a Cary model 83 GT or a Spex model 1403 spectrophotometer using the 488-nm exciting line of an Ar ion or the 647.1-nm line of a Kr ion laser, respectively. A previously described[18] device was used for the recording of the low-temperature spectra.

Preparation of M_2BiF_7 (M = Na, K, Rb, Cs). In a typical experiment, finely powdered dry KF (21.0 mmol) and BiF_5 (7.0 mmol) were loaded inside the drybox into a prepassivated (with ClF_3) 75-mL Monel reactor which was closed by a Monel valve. On the metal vacuum line, the reactor was evacuated, and gaseous fluorine (300 Torr) was added. The reactor was heated in an electrical oven to 250 °C for 4 days. The reactor was removed from the oven, and the fluorine gas was pumped off. The white solid product (3349 mg, mass calcd for 7.0 mmol of K_2BiF_7 and 7.0 mmol of KF = 3348 mg) was shown by vibrational spectroscopy to be a mixture of K_2BiF_7 and KF and did not contain any amounts of $KBiF_6$ or unreacted BiF_5, detectable by Raman spectroscopy. Using only a 2:1 mole ratio of MF:BiF_5 and lower reaction temperatures and shorter reaction times, BiF_7^{2-} salts were still the major products but frequently contained some $MBiF_6$ impurities. For the synthesis of Cs_2BiF_7, a 3:1 mole ratio of CsF:BiF_5 and a reaction temperature of 310 °C for 4 days gave a product that was essentially free of BiF_6^-.

Preparation of $[N(CH_3)_4]_2BiF_7$. In the drybox, a prepassivated (with ClF_3) $^3/_4$-in.-o.d. Teflon−FEP ampule, which was equipped with a Teflon-coated magnetic stirring bar and was closed by a stainless steel valve, was loaded with anhydrous $N(CH_3)_4F$ (1.93 mmol). On the glass vacuum line, dry CH_3CN (5.754 g) was added at −196 °C, and the mixture was warmed to room temperature to dissolve the $N(CH_3)_4F$. The ampule was cooled to −196 °C, and BiF_5 (0.961 mmol) was added to the cold ampule inside the drybox. The ampule was reconnected to the glass line and warmed to −31 °C for 100 min with stirring. Upon melting of the CH_3CN, a yellow color was observed, followed by the formation of a light yellow precipitate. The CH_3CN solvent was pumped off at −22 °C in a dynamic vacuum, leaving behind 499 mg (mass calcd for 0.961 mmol of $[N(CH_3)_4]_2BiF_7$ = 471 mg) of a light yellow solid which, based on its vibrational spectra, contained mainly the BiF_7^{2-} and $N(CH_3)_4^+$ ions,[15,19] in addition to some small amounts of BiF_6^- and some HF_2^- and $H_2F_3^-$,[19] which can account for the extra weight.

Preparation of $(NO)_2BiF_7$. In a typical experiment, BiF_5 (1.618 mmol) was loaded in the drybox into a prepassivated $^3/_4$-in.-o.d. Teflon-FEP ampule which contained a Teflon-coated magnetic stirring bar and was closed with a stainless steel valve. On the metal vacuum line, FNO (23.83 mmol) was added at −196 °C, and the mixture was stirred for 24 h at −78 °C. The excess of unreacted FNO (21 mmol) was pumped off at −78 °C, leaving behind a white solid which was shown by low-temperature Raman spectroscopy to be a mixture of (NO_2)-BiF_7 and unreacted BiF_5 [596(100), 569(10), 252(8), 165(7)br, in good agreement with a previous report[20]]. On warming to room temperature in a dynamic vacuum, the solid lost half of its FNO content, leaving behind $NOBiF_6$ [Ra at 25 °C: NO^+, ν = 2338(5); BiF_6^-, $\nu_1(A_{1g})$ = 590(100), $\nu_2(E_g)$ = 547(3) and 519(11), $\nu_5(F_{2g})$ = 247(13), 231(10) and 212(2)] and unreacted BiF_5.

Preparation of M_2SbF_7 (M = K, Cs, $N(CH_3)_4$). The procedures and reaction conditions were analogous to those described above for M_2BiF_7, except for using SbF_5 in place of BiF_5. With a mole ratio of MF:SbF_5 of 3:1 and heating for 4 days to 250 °C, the mole ratio of SbF_7^{2-}:SbF_6^- in the product was about 3:1. However, heating of a mixture of $CsSbF_6$ and CsF in a mole ratio of 1:2 to 300 °C for 45 h resulted in essentially complete conversion of $CsSbF_6$ to Cs_2SbF_7.

A mixture of $CsSbF_6$ and CsF in a mole ratio of 1:2, together with two steel balls, was placed into the stainless steel cup of a high-frequency "Wig-L-Bug" shaker, normally used for the preparation of samples for infrared spectroscopy. The Raman spectrum of the mixture after 1 h of vigorous shaking at room temperature showed a conversion of SbF_6^- to SbF_7^{2-} of about 13%.

Reactions of Cs_2XF_7 (X = Bi, Sb) with Anhydrous HF. Samples of 1:1 mixtures of Cs_2BiF_7/CsF or Cs_2SbF_7/CsF, when treated with a large excess of anhydrous HF at room temperature, were converted to $CsXF_6$ and $2CsHF_2$, as shown by mass balance and vibrational spectroscopy.

Computational Methods. Quantum-chemical calculations employing the Hartree−Fock (HF) self-consistent-field and Møller−Plesset second-order perturbation theory (MP2) methods were performed for the free D_{5h} symmetry BiF_7^{2-} compound in several atomic basis sets, yielding equilibrium structures and vibrational spectra. To calibrate the methods and basis sets, analogous calculations were carried out on the well-characterized and closely related octahedral BiF_6^- anion. Basis set 1 was comprised of a double-ζ plus polarization (DZP) basis on fluorine atoms,[21] with DZP basis sets for the valence shells and effective core potentials (ECP) for the inner shells of bismuth.[22] Basis set 2 consisted of the 6-311G(d) fluroine basis[23] and the LANL2DZ[22,24] bismuth ECP/valence-DZ basis supplemented with a d function having an exponent of 0.185 on bismuth. Basis set 3 was comprised of the SBKJC valence-double-ζ and ECP sets for both fluorine and bismuth atoms,[24−26] supplemented with d functions having exponents of 0.80 and 0.185, respectively, and with diffuse s and p functions with common exponents of 0.1076 and 0.0215, respectively. Basis set 4 was simply basis 2 supplemented with diffuse s and p functions having common exponents of 0.1288 and 0.0515 for fluorine and 0.0298 for bismuth. And finally, basis set 5, comprised from elements of sets 3 and 4, can be succinctly summarized as F:6-311G(d; sp = 0.1288, 0.0515)/Bi: SBJKC(d = 0.185; sp = 0.01857). Based on results obtained for BiF_6^- and BiF_7^{2-}, basis sets 1, 3, and 5 were chosen for use in HF and MP2 calculations on the analogous arsenic and antimony compounds.

Harmonic vibrational frequencies and infrared intensities were computed on the basis of analytic first and numerical second derivatives of the molecular energy and first derivatives of the dipole moment with respect to nuclear coordinates at all levels of calculation. Calculations employed the GRADSCF,[27] GAMESS,[28] and Gaussian[29] program systems. The calculated Hessian matrixes (second derivatives of the

(16) Christe, K. O.; Schack, C. J. *Inorg. Chem*. **1970**, *9*, 1852.
(17) Christe, K. O.; Wilson R. D.; Schack, C. *J. Inorg. Synth*. **1986**, *24*, 3.
(18) Miller, F. A.; Harney, B. M. *Appl. Spectrosc*. **1969**, *23*, 8.
(19) Wilson, W. W.; Christe, K. O.; Feng, J.; Bau, R. *Can. J. Chem*. **1989**, *67*, 1898.
(20) Beattie, I. R.; Livingston, K. M. S.; Ozin, G. A.; Reynolds, D. J. *J. Chem. Soc. (A)* **1969**, 958. Beattie, I. R.; Cheetham, N.; Gilson, T. R.; Livingston, K. M. S.; Reynolds, D. J. *J. Chem. Soc. (A)* **1971**, 1910.
(21) Dunning, T. H., Jr.; Hay, P. J. In *Methods of Electronic Structure Theory*; Schaefer, H. F., III, Ed.; Plenum: New York, 1977; Chapter 1.
(22) Wadt, W. R.; Hay, P. J. *J. Chem. Phys*. **1985**, *82*, 284.
(23) Krishnan, R.; Binkley, J. S.; Seeger, R.; Pople, J. A. *J. Chem. Phys*. **1980**, *72*, 650.
(24) Stevens, W. J.; Basch, H.; Krauss, M. *J. Chem. Phys*. **1984**, *81*, 6026.
(25) Stevens, W. J.; Krauss, M.; Basch, H.; Jasien, P. G. *Can. J. Chem*. **1992**, *70*, 612.
(26) Basis sets and some of the terminology used here were obtained from the Gaussian Basis Set Library, developed and distributed by the Environmental and Molecular Sciences Laboratory of Pacific Northwest National Laboratory, accessible on the World Wide Web at universal resource locator http://www.emsl.pnl.gov: 2080/forms/basisform.html.
(27) GRADSCF is an ab initio quantum chemistry program system designed and written by A. Komornicki, Polyatomics Research Institute, Redwood City, CA.
(28) Schmidt, M. W.; Baldridge, K. K.; Boatz, J. A.; Elbert, S. T.; Gordon, M. S.; Jensen, J. H.; Koseki, S.; Matsunaga, N.; Nguyen, K. A.; Su, S. J.; Windus, T. L.; Dupuis, M.; Montgomery, J. A. *J. Comput. Chem*. **1993**, *14*, 1347.

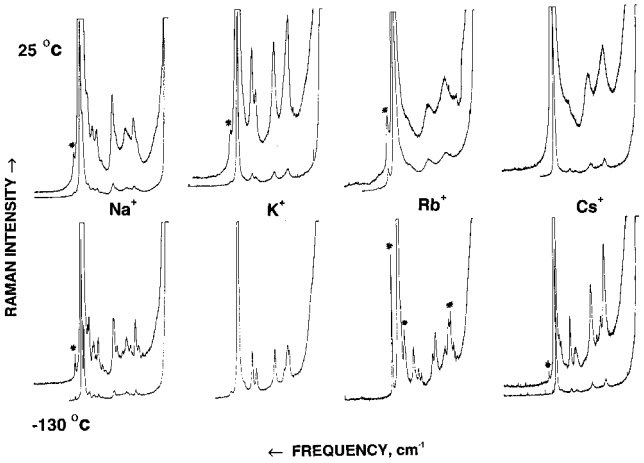

Figure 1. Raman spectra of solid Na_2BiF_7, K_2BiF_7, Rb_2BiF_7, and Cs_2BiF_7, recorded at 25 and −130 °C. Bands masked by an asterisk are due to BiF_6^-. The frequencies are listed in Table 1.

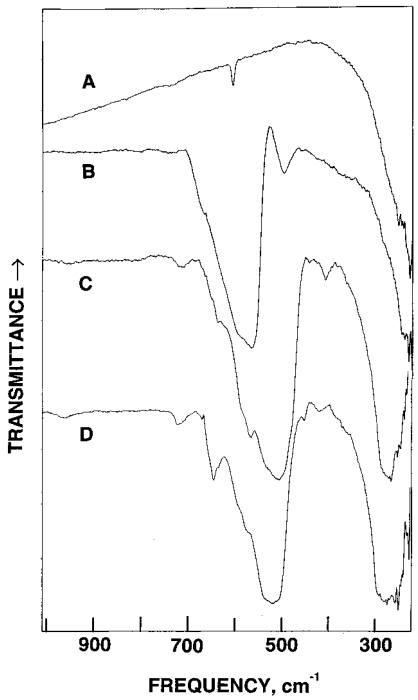

Figure 2. Room-temperature infrared spectra of pressed AgBr disks of the following solids: (A) CsF; (B) $CsBiF_6$; (C) Cs_2BiF_7, containing small amounts of $CsBiF_6$ and CsF; and (D) Cs_2BiF_7, containing about 50% CsF and a trace of $CsBiF_6$.

energy with respect to Cartesian coordinates) were converted to symmetry-adapted internal coordinates for further analysis using the program systems GAMESS and Bmtrx.[30]

Results and Discussion

Syntheses and Properties of BiF_7^{2-} Salts. The syntheses of the Na^+, K^+, Rb^+, and Cs^+ salts of BiF_7^{2-} are surprisingly simple and were achieved by heating BiF_5 with an excess of the corresponding alkali metal fluoride to temperatures above 230 °C for several days in a Monel reactor (eq 1).

$$2MF + BiF_5 \xrightarrow{230-310\ °C} M_2BiF_7 \quad (M = Na, K, Rb, Cs) \qquad (1)$$

To preempt a possible reduction of Bi(+V) to Bi(+III), a low pressure of gaseous F_2 was used as a protective gas during the

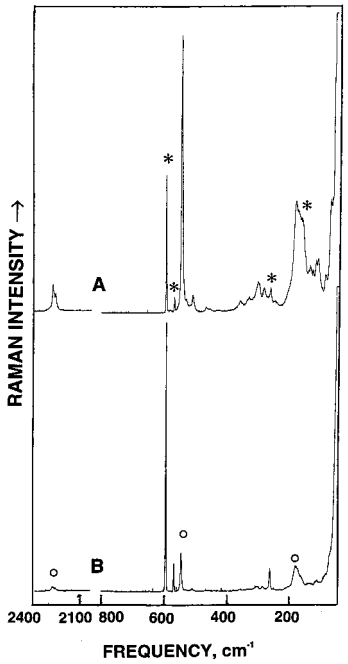

Figure 3. Raman spectra of $(NO)_2BiF_7$ recorded at −130 °C. (A) Spectrum of mainly $(NO)_2BiF_7$ containing a small amount of BiF_5, which is marked by asterisks. (B) Spectrum of mainly BiF_5 containing a small amount of $(NO)_2BiF_7$, which is marked by a circle.

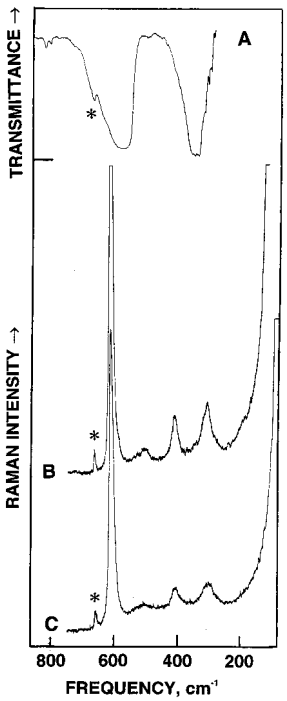

Figure 4. Vibrational spectra of Cs_2SbF_7. (A) Infrared spectrum of an AgBr disk recorded at room temperature. (B and C) Raman spectra recorded at −130 and 25 °C, respectively. The bands marked by an asterisk are attributed to a small amount of SbF_6^-.

(29) Frisch, M. J.; Trucks, G. W.; Schlegel, H. B.; Gill, P. M. W.; Johnson, B. G.; Robb, M. A.; Cheeseman, J. R.; Keith, T.; Petersson, G. A.; Montgomery, J. A.; Raghavachari, K.; Al-Laham, M. A.; Zakrzewski, V. G.; Ortiz, J. V.; Foresman, J. B.; Cioslowski, J.; Stefanov, B. B.; Nanayakkara, A.; Challacombe, M.; Peng, C. Y.; Ayala, P. Y.; Chen, W.; Wong, M. W.; Andres, J. L.; Replogle, E. S.; Gomperts, R.; Martin, R. L. Fox, D. J.; Binkley, J. S.; Defrees, D. J.; Baker, J.; Stewart, J. P.; Head-Gordon, M.; Gonzalez, C.; Pople, J. A. *Gaussian 94*, Revision E.2; Gaussian, Inc.: Pittsburgh, PA, 1995.

(30) Komornicki, A. *Bmtrx*, Version 2.0; Polyatomics Research Institute: Redwood City, CA, 1996.

Table 1. Observed Vibrational Spectra of the BiF_7^{2-} Dianion

				obsd freq, cm^{-1} (rel intens)														
				Na_2BiF_7			K_2BiF_7			Rb_2BiF_7			Cs_2BiF_7			$[N(CH_3)_4]_2BiF_7$		$(NO)_2Bi_7$[c]
				Ra		IR,	Ra		IR,	Ra		IR,	Ra		IR,	Ra,	IR,	Ra,
IR−Ra activity	assignment in point group D_{5h}		approximate mode description	−130 °C	25 °C	25 °C	−130 °C	25 °C	25 °C	−130 °C	25 °C	25 °C	−130 °C	25 °C	25 °C	25 °C	25 °C	−130 °C
−Ra	A_1'	ν_1	νsym BiF_5	561(100)	561(100)		553(100)	549(100)		548(100)	543(100)		540(100)	536(100)		538(100)		546(100)
				549(47)	551(40)													
		ν_2	νsym BiF_2	526(3)	520(2)		516(1)	520sh		530(6)	510sh		519(1)	520sh				530sh
				519(4)						511(6)			509(1)	505(2)				509(5)
IR−	A_2''	ν_3	νasym BiF_2												(515vs,br)[a]			
		ν_4	δumbrella BiF_5												(287vs,br)[b]			
IR−	E_1'	ν_5	νasym BiF_5			534vs			528vs, br			525vs, br			515vs,br		508s	
		ν_6	δasym BiF_5 in-plane						280vs									
		ν_7	δsciss BiF_2												287vs,br			
−Ra	E_1''	ν_8	δwag BiF_2	299(1)	299(1)		284sh			279(3)			299(0.5)	295(0+)				295(12)
				278(0.5)			267(5)			259(5)	273sh		276(1)	270(1)				277(6)
				251(2)	254(2)		255(4)	252(6)		249(6)	249(11)		250(6)	247(6)				
				233(0.5)	235sh		240sh			229(2)				238sh				
−Ra	E_2'	ν_9	δasym BiF_5 in-plane	495(0.5)														
				490(1)	490(2)		469(5)	460(4)	463w	459(5)	452(4)	458vw	454(3)	450(3)				465(2)
				478(0.3)	466(2)	465vw	444(3)	438(2)		430(2)	427(2)		431(0.5)	419(1)				453(1)
				465(2)						413(2)			424(1)	409(1)				436(1)
		ν_{10}	νasym BiF_5	376(3)	375(4)		340(5)	332(5)		350(3)	350sh		331(4)	326(4)				353(4)
				354(0.5)	358sh					331(6)	330(7)							329(2)
−Ra	E_2''	ν_{11}	δpucker BiF_5															

[a] The ν_3 band is probably hidden underneath the very strong and broad ν_5 band. [b] The ν_4 band is probably hidden underneath the very stong and broad ν_6 band. [c] In addition to the listed BiF_7^{2-} vibrations, the following bands were observed: 2280(9) and 2260(5), νNO^+; 172(37,br), 125(3), 106(2), 99(9), 73(3), and 58(3), which are tentatively assigned to cation−anion interactions and/or lattice modes.

Table 2. Observed and Calculated Vibrational Spectra of the SbF_7^{2-} Dianion

assignment in point group D_{5h}		obsd freq, cm^{-1} (rel intens)						unscaled calcd freq cm^{-1} (IR intens)[a]	
		K_2SbF_7			Cs_2SbF_7				
		Ra			Ra				
		−130 °C	25 °C	IR, 25 °C	−130 °C	25 °C	IR, 25 °C	HF/1	HF/5
A_1'	ν_1	605(100)	604(100)		596(100)	597(100)		608(0)	602(0)
	ν_2	520(7)	517(6)		512(1)	520sh		527(0)	522(0)
A_2''	ν_3						627sh	640(193)	635(199)
	ν_4							345(107)	342(107)
E_1'	ν_5			585vs,br			574vs	559(346)	551(185)
	ν_6			342vs,br			335vs	392(366)	384(201)
	ν_7							232(7)	233(2)
E_1''	ν_8	294(17)	297(20)		289(6)	285(5)		293(0)	292(0)
E_2'	ν_9	495(6)	495(4)		490(1.5)	492(2)br		501(0)	491(0)
	ν_{10}	396(7)	395(5)		392(5)	391(5)		377(0)	369(0)
E_2''	ν_{11}							34(0)	64(0)

[a] For basis sets, see text.

Table 3. Comparison of Experimental Frequencies (cm^{-1}) of BiF_7^{2-} and the Isoelectronic Series, IF_7, TeF_7^-, SbF_7^{2-}

		IF_7[a]	TeF_7^- [b]	SbF_7^{2-} [c]	BiF_7^{2-} [c]
A_1'	ν_1	676	640	596	545
	ν_2	635	597	512	510
A_2''	ν_3	746	699	627	
	ν_4	365	335	(300)[d]	
E_1'	ν_5	670	625	574	520
	ν_6	425	385	335	284
	ν_7	257			
E_1''	ν_8	319	295	289	260
E_2'	ν_9	596	(540)[d]	490	460
	ν_{10}	510	458	392	330
E_2''	ν_{11}				

[a] Data from ref 39. [b] Data from ref 40. [c] Data from this study. [d] Predicted values, based on the trends observed in this table.

heating. However, excessive heating and significant fluorine pressures must be avoided, as they can result in attack of the Monel cylinder with the formation of some NiF_6^{2-} impurities, which can be easily detected by their pink color and intense Raman bands at about 560, 519, and 294 cm^{-1}. To suppress the simultaneous formation of some BiF_6^- salts, it is advantageous to use a 50% molar excess of the alkali metal fluorides. Even with a large excess of alkali metal fluoride, there was no evidence for the formation of BiF_8^{3-} salts under these conditions. Attempts to prepare Li_2BiF_7 under similar conditions were also unsuccessful. The lack of Li_2BiF_7 formation is not surprising in view of the previous findings that the tendency of alkali metal fluorides to form stable complex fluoroanion salts with covalent main group fluorides or oxofluorides decreases from Cs^+ to Li^+. The main driving forces for salt formation are the fluoride ion affinities of the covalent main group fluorides and the lattice energy differences between the fluorides and the complex fluoroanion salts of the alkali metals. Without exact knowledge of these values, it is difficult to predict exactly where the cutoff limit for salt formation lies for a given system and can vary somewhat from one system to another. Thus, SbF_5,[13] BiF_5,[14] and IF_3O [31] can form stable Li^+, Na^+, K^+, Rb^+ and Cs^+ salts of SbF_6^-, BiF_6^-,and IF_5O^-, respectively, while BiF_3,[32] SeF_4,[33] and SeF_6[34] form only stable Na^+, K^+, Rb^+, and Cs^+ salts, and ClF,[35] ClF_3,[36] ClF_3O,[37] and IF_5[38] form only stable K^+, Rb^+, and Cs^+ salts.

By analogy to the halogen (see above) or xenon fluorides or oxofluorides,[31−38] BiF_5 also forms at −78 °C a thermally unstable $(NO)_2BiF_7$ salt (eq 2a) which, on warming to room temperature, loses 1 mol of FNO to give stable $NO^+BiF_6^-$ (eq 2b).

$$2FNO + BiF_5 \xrightarrow[FNO(liq)]{-78\ ^\circ C} (NO)_2BiF_7 \qquad (2a)$$

$$(NO)_2BiF_7 \xrightarrow[vac]{25\ ^\circ C} NOBiF_6 + FNO \qquad (2b)$$

A stable $[N(CH_3)_4]_2BiF_7$ salt was also prepared. Due to the limited thermal stability and oxidizer resistance of $N(CH_3)_4F$,[15] a thermal synthesis at 250 °C was not feasible, and a low-temperature synthesis in CH_3CN solution had to be employed (eq 3).

$$2N(CH_3)_4F + BiF_5 \xrightarrow[CH_3CN]{-31\ ^\circ C} [N(CH_3)_4]_2BiF_7 \qquad (3)$$

Removal of the CH_3CN solvent at −22 °C resulted in a product which contained mainly $[N(CH_3)_4^+]_2BiF_7$ but also some smaller amounts of $N(CH_3)_4^+$ salts of BiF_6^-, HF_2^-, and $H_2F_3^-$, with the bifluoride anions being generated by hydrogen abstraction from CH_3CN by either F^- [19] or the bismuth fluorides.

The alkali metal BiF_7^{2-} salts are thermally stable, crystalline, white solids which exhibit little solubility in convential organic solvents. Attempts to dissolve the compounds in anhydrous HF, resulted in the following displacement reaction (eq 4).

$$M_2BiF_7 + HF \xrightarrow[25\ ^\circ C]{HF} MHF_2 + MBiF_6 \qquad (4)$$

Similarly, when $N(CH_3)_4F$ and SbF_5 in a 2.2:1 mole ratio were combined at −45 °C in SO_2 solution, only $N(CH_3)_4^+SbF_6^-$ and $N(CH_3)_4^+SO_2F^-$ were obtained in quantitative yield. This indicates that, in SO_2 solution, these heptafluoropnictate(V) dianions also undergo solvolysis (eq 5).

(31) Christe, K. O.; Wilson, W. W.; Wilson, R. D. *Inorg. Chem.* **1989**, *28*, 904.
(32) (a) Stein, L. In *Halogen Chemistry*; Gutmann, V., Ed.; Academic Press: New York, 1967; Vol. 1, p 133. (b) Rhein, R. A.; Miles, M. H. Technical Report 6811; Naval Weapons Center: China Lake, CA, 1988.
(33) Christe, K. O.; Curtis, E. C.; Dixon, D. A.; Mercier, H. P.; Sanders, J. C. P. Schrobilgen, G. J. *J. Am. Chem. Soc.* **1991**, *113*, 3351.
(34) Christe, K. O.; Wilson, W. W. *Inorg. Chem.* **1982**, *21*, 4113.
(35) Christe, K. O.; Guertin, J. P. *Inorg. Chem.* **1965**, *4*, 1785.
(36) (a) Christe, K. O.; Wilson, W. W.; Wilson, R. D. *Inorg Chem.* **1989**, *28*, 675. (b) Wilson, W. W.; Christe, K. O. *Inorg. Chem.* **1989**, *28*, 4172 and references therein.
(37) Christe, K. O.; Schack, C. J.; Pilipovich, D. *Inorg. Chem.* **1972**, *11*, 2205.
(38) Christe, K. O. *Inorg. Chem.* **1972**, *11*, 1215.

Table 4. Unscaled Calculated[a] Vibrational Frequencies (cm^{-1}) and IR Intensities (km/mol) of D_{5h} BiF_7^{2-}

assignment		HF/1	HF/2	MP2/2	HF/3	MP2/3	HF/4	MP2/4	HF/5	MP2/5
A_1'	ν_1	568(0)	581(0)	511(0)	579(0)	482(0)	572(0)	483(0)	565(0)	474(0)
	ν_2	502(0)	521(0)	489(0)	495(0)	445(0)	505(0)	458(0)	490(0)	447(0)
A_2''	ν_3	576(166)	582(144)	532(125)	578(173)	495(181)	573(164)	502(153)	561(167)	490(157)
	ν_4	287(106)	295(115)	271(84)	289(106)	254(98)	292(115)	261(80)	289(113)	256(76)
E_1'	ν_5	527(298)	547(279)	501(226)	510(301)	448(325)	525(313)	465(276)	516(308)	454(136)
	ν_6	337(300)	340(298)	314(223)	330(351)	291(322)	329(340)	295(254)	327(342)	291(125)
	ν_7	197(15)	203(15)	187(10)	204(13)	179(9)	206(10)	185(6)	203(10)	180(3)
E_1''	ν_8	255(0)	263(0)	242(0)	261(0)	230(0)	262(0)	233(0)	260(0)	231(0)
E_2'	ν_9	456(0)	462(0)	434(0)	456(0)	397(0)	448(0)	403(0)	442(0)	396(0)
	ν_{10}	387(0)	404(0)	381(0)	352(0)	331(0)	375(0)	348(0)	364(0)	341(0)
E_2''	ν_{11}	46i	24i	18i	17i	9i	25(0)	6i	32(0)	32(0)

[a] For a description of the basis sets used, see text.

$$SbF_7^{2-} + SO_2 \xrightarrow{SO_2} SbF_6^- + SO_2F^- \quad (5)$$

The hydrolysis of BiF_7^{2-} salts is analogous to that of BiF_6^-;[14] i.e., the white solids first turn yellow when exposed to moist air and, when added to water, first form yellow solutions which, after several minutes, turn dark brown due to the formation of high-oxidation-state bismuth oxides. The only difference from BiF_6^- salts is that, while for BiF_6^- these reactions are practically instantaneous, for BiF_7^{2-} they take several minutes to proceed; i.e., the increased coordination sphere around the central atom and the double negative charge of the dianions apparently retard the attack by OH^- ions.

The M_2BiF_7 salts were shown by Raman spectroscopy (see below) to be distinct compounds containing the BiF_7^{2-} anion and not mixtures of BiF_6^- and F^- ions. Based on their preparative conditions, the Na^+, K^+, Rb^+, and Cs^+ salts of BiF_7^{2-} are thermally stable up to at least 300 °C. The thermal stability of $[N(CH_3)_4]_2BiF_7$ is limited by the stability of the organic cation, which, as in $N(CH_3)_4F$,[19] is prone to lose CH_3F on pyrolysis.

Syntheses and Properties of SbF_7^{2-} Salts. Antimony pentafluoride is also capable of forming a stable dianion with excess alkali metal fluorides. However, contrary to BiF_5, SbF_5 does not form a stable sodium salt, and only salts with potassium or heavier alkali metals are obtainable. The salts were prepared by heating either SbF_5 with excess KF or CsF to 220−300 °C (eq 6a) or, preferably, $CsSbF_6$ with 2 mol of CsF to 300 °C (eq 6b).

$$2MF + SbF_5 \xrightarrow{220-300\ °C} M_2SbF_7 \quad (M = K, Cs) \quad (6a)$$

$$CsSbF_6 + CsF \xrightarrow{300\ °C} Cs_2SbF_7 \quad (6b)$$

Surprisingly, it was found that $CsSbF_6$, when ball-milled for 1 h at room temperature in a high-frequency Wig-L-Bug, showed a 13% conversion to Cs_2SbF_7, indicating that the activation energy barrier toward SbF_7^{2-} formation is low. The heat required for the thermal syntheses of these salts probably serves only the purpose of increasing the ion mobilities and might involve melting or volatilization of either the starting materials or the reaction products.

The alkali metal SbF_7^{2-} salts, like their BiF_7^{2-} analogues, are stable, white, crystallinic solids with little solubility in organic solvents. In inorganic solvents, such as HF or SO_2, they readily undergo solvolysis accompanied by loss of one F^- ion (see above), thus foiling their study by NMR spectroscopy.

Antimony pentafluoride also forms a stable $[N(CH_3)_4]_2SbF_7$ salt, which was prepared by analogy to the BiF_7^{2-} salt at −31 °C in CH_3CN solution. However, low-temperature Raman spectroscopy failed to provide any evidence for the formation of $(NO)_2SbF_7$ in the SbF_5/FNO system at −78 °C, with $NO^+SbF_6^-$ being the only observable product.

Attempted Synthesis of AsF_7^{2-} Salts. Attempts to prepare Cs_2AsF_7 by heating AsF_5 with a 3-fold excess of CsF for 4 days to 230 °C produced exclusively $CsAsF_6$. Similarly, reactions of AsF_5 with excess $N(CH_3)_4F$ in CH_3CN at −31 °C gave no evidence for the formation of $[N(CH_3)_4]_2AsF_7$.

Although the ab initio calculations (see below) predict that the free gaseous AsF_7^{2-} ion is vibrationally stable toward F^- loss, the formation of stable solid AsF_7^{2-} salts appears to be energetically unfavorable relative to that of $MAsF_6$ and MF. Thus, the propensity of pnicogen pentafluorides to form heptafluoro dianions decreases in the order $BiF_5 > SbF_5 > AsF_5$, as expected from the decreasing size of the central atom and the decreasing F^- ion affinity of the pentafluorides.

Vibrational Spectra. In the absence of single-crystal X-ray and NMR data, a combination of vibrational spectroscopy and ab initio calculations was used to characterize these novel heptacoordinated dianions. The observed Raman and infrared spectra are shown in Figures 1−4, and their frequencies and assignments have been summarized in Tables 1 and 2. Based on the results from the ab initio calculations (see below) and a comparison with the known spectra of isoelectronic pentagonal bipyramidal IF_7[39] and TeF_7^- [40] (see Table 3), the observed spectra are assigned in point group D_{5h} and establish the pentagonal bipyramidal structures of BiF_7^{2-} and SbF_7^{2-}.

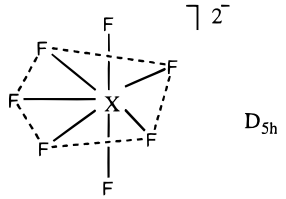

As can be seen from Figure 1 and Table 1, the spectra of BiF_7^{2-} are significantly influenced by the counterion. By analogy with previous findings for different alkali metal salts of IF_4O^- [1] and BrF_4O^-,[41] the band splittings increase with decreasing cation size, and the frequencies vary slightly from salt to salt, in accord with increasing anion−cation interactions. Additional evidence for increased cation−anion interaction with decreasing cation size comes from the Raman spectrum of $(NO)_2BiF_7$ (see Table 1 and Figure 3). Whereas the BiF_7^{2-}

(39) Christe, K. O.; Curtis, E. C.; Dixon, D. A. *J. Am. Chem. Soc.* **1993**, *115*, 1520 and references therein.
(40) Christe, K. O.; Dixon, D. A.; Sanders, J. C. P.; Schrobilgen, G. J.; Wilson, W. W. *J. Am. Chem. Soc.* **1993**, *115*, 9461.
(41) Christe, K. O.; Wilson, R. D.; Curtis, E. C.; Kuhlmann, W.; Sawodny, W. *Inorg. Chem.* **1978**, *17*, 533.
(42) Marx, R.; Mahjoub, A. R.; Seppelt, K.; Ibberson, R. M. *J. Chem. Phys.* **1994**, *101*, 585.

frequencies are comparable with those in the alkali metal salts, the NO^+ stretching frequency (2280 and 2260 cm^{-1}) has decreased approximately 70 cm^{-1} from that (2338 cm^{-1}) found for the more ionic $NO^+BiF_6^-$ salt (see Experimental Section).

Furthermore, the Raman spectra exhibit a very pronounced temperature dependence, as is expected for highly fluxional pentagonal bipyramidal species.[39,40] At room temperature, they undergo a rapid dynamic puckering of the highly congested equatorial plane and a slower intramolecular exchange of the axial and equatorial fluorine ligands.[39] This causes the room-temperature Raman bands to become very broad and to lose most of their fine structure.

Recording reliable infrared spectra in the low-frequency range was somewhat problematic since an excess of alkali metal fluoride, which also absorbs in this range, had to be used in the syntheses to suppress the formation of the octahedral XF_6^- monoanions. With the heaviest alkali metal fluoride, i.e., CsF, the 290-cm^{-1} IR band could still be well established (see Figure 2). However, for the lighter alkali metal fluorides, which start to absorb already at higher frequencies, some interference with the XF_7^{2-} deformation modes was encountered. For the SbF_7^{2-} salts this was less of a problem than for BiF_7^{2-}, because the ν_6 antisymmetric deformation mode of SbF_7^{2-} occurs at a higher frequency ($\sim$335 cm^{-1}). However, the similar frequencies of ν_3 and ν_5 and ν_4 and ν_6 and the broadness of their infrared bands rendered the observation of ν_3 and ν_4 somewhat uncertain. As can be seen from Figure 4, the ν_5 infrared band of SbF_7^{2-} exhibits in the region expected for ν_3 a shoulder at 627 cm^{-1} and a weak band at 660 cm^{-1}. Since the latter frequency coincides with ν_3 of SbF_6^- and the Raman spectrum established the presence of a small amount of SbF_6^- in our sample, the 627-cm^{-1} shoulder is assigned to ν_3 of SbF_7^{2-}. Similarly, there are several shoulders on the low-frequency side of the 335-cm^{-1} ν_6 band of SbF_7^{2-}, and one of these could be due to ν_4 of SbF_7^{2-}.

Electronic Structure Calculations and Vibrational Assignments. The well-known and closely related octahedral BiF_6^-, SbF_6^-, and AsF_6^- anions were used to test the different methods and basis sets used in our calculations. As can be seen from Table 5, the Hartree−Fock calculations with basis Sets 1 and 5, denoted as HF/1 and HF/5, gave the best agreement with the observed frequencies and geometries and were, therefore, preferentially used for all the other calculations in this study.

In agreement with the known experimental D_{5h} structures of isoelectronic IF_7[39,42] and TeF_7^-,[10,40] our ab initio calculations for BiF_7^{2-}, SbF_7^{2-}, and AsF_7^{2-} result in pentagonal bipyramids of D_{5h} symmetry (see Table 6) as the minimum energy structures. Within the isoelectronic series XeF_7^+, IF_7, TeF_7^-, and SbF_7^{2-}, the energy differences between the pentagonal bipyramidal (PBP) structure and the monocapped trigonal prismatic (MCTP) and monocapped octahedral (MCO) structures were calculated at the MP2 level to be about 3−4 kcal/mol, with the differences between the MCTP and the MCO structures being very small, favoring the MCTP by about 0.2 kcal/mol. Assuming similar bond length deviations as for BiF_6^-, SbF_6^-, and AsF_6^- (see Table 5), the most likely geometries of BiF_7^{2-}, SbF_7^{2-}, and AsF_7^{2-} can be predicted and are summarized in Table 6. The calculated frequencies of BiF_7^{2-}, SbF_7^{2-}, and AsF_7^{2-} are summarized in Tables 4 and 7, 2 and 8, and 9, respectively. The imaginary frequencies found for ν_{11} of BiF_7^{2-} in some of the calculations, given in Table 4, are probably due to the numerical differentiation used in our calculations and can be avoided by appropriate modification of the basis set (see Table 4).

Table 5. Observed and Unscaled Calculated Vibrational Frequencies (cm^{-1}) and Geometries (Å) for Octahedral BiF_6^-, SbF_6^-, and AsF_6^-

		BiF_6^-								SbF_6^-						AsF_6^-					
			calcd[d]							calcd[d]											
mode	sym	obsd[a]	HF/1	HF/2	HF/3	HF/4	HF/5	MP2/2	MP2/3	MP2/4	MP2/5	obsd[b]	HF/1	HF/3	HF/5	MP2/3	MP2/5	obsd[c]	HF/1	HF/3	HF/5	MP2/3	MP2/5
ν_1	A_{1g}	590	617(0)[e]	632(0)	649(0)	627(0)	621(0)	561(0)	549(0)	541(0)	535(0)	648	667(0)	681(0)	662(0)	603(0)	588(0)	689	729(0)	734(0)	712(0)	635(0)	622(0)
ν_2	E_g	520	557(0)	577(0)	572(0)	564(0)	550(0)	545(0)	514(0)	520(0)	509(0)	569	585(0)	589(0)	584(0)	539(0)	538(0)	576	612(0)	607(0)	597(0)	550(0)	543(0)
ν_3	F_{1u}	580	625(423)	631(350)	632(442)	622(406)	611(402)	580(274)	551(447)	556(344)	544(345)	665	683(502)	690(533)	679(172)	622(547)	619(158)	698	760(698)	756(762)	754(258)	675(781)	680(234)
ν_4	F_{1u}	215	271(285)	272(306)	277(290)	277(311)	275(312)	252(227)	247(274)	250(228)	247(223)	280	331(315)	339(298)	334(106)	306(286)	307(83)	391	442(278)	446(264)	438(91)	394(240)	393(68)
ν_5	F_{2g}	237	266(0)	268(0)	273(0)	276(0)	273(0)	247(0)	243(0)	245(0)	244(0)	275	308(0)	318(0)	312(0)	285(0)	282(0)	376	396(0)	403(0)	392(0)	354(0)	349(0)
ν_6	F_{2u}		153(0)	160(0)	161(0)	168(0)	164(0)	149(0)	143(0)	152(0)	148(0)		187(0)	195(0)	196(0)	173(0)	179(0)		261(0)	264(0)	260(0)	230(0)	232(0)
bond length		1.92[f]	1.920	1.931	1.921	1.930	1.932	1.977	1.978	1.985	1.989	1.86[g]	1.852	1.841	1.858	1.889	1.901	1.72[h]	1.710	1.709	1.720	1.757	1.764

[a] Averaged frequencies taken from different salts of refs 14 and 43. [b] Averaged values from refs 13 and 44. [c] Averaged values from ref 45 and our own work. [d] For basis sets see text. [e] Infrared intensities in km/mol. [f] Averaged value from ref 46. [g] Averaged value from refs 43 and 47. [h] Value from ref 48.

Table 6. Calculated and Predicted Geometries for the D_{5h} BiF_7^{2-}, SbF_7^{2-}, and AsF_7^{2-} Dianions[a]

	calcd[b] (predicted) bond lengths (Å)										
	BiF_7^{2-}							SbF_7^{2-}		AsF_7^{2-}	
	HF/1	HF/2	HF/3	HF/4	HF/5	MP2/2	MP2/5	HF/1	HF/5	HF/1	HF/5
$rX-F_{ax}$	1.951	1.958	1.945	1.957	1.945	2.010	2.024 (1.96)	1.875	1.878 (1.89)	1.718	1.723 (1.74)
$rX-F_{eq}$	2.008	2.009	2.009	2.016	2.009	2.055	2.081 (2.03)	1.953	1.959 (1.97)	1.847	1.861 (1.87)

[a] For D_{5h} symmetry, all bond angles are the same: $\angle F_{eq}XF_{eq} = 72°$ and $\angle F_{ax}XF_{eq} = 90°$. [b] For basis sets, see text.

Table 7. Unscaled HF/DZP/ECP (HF/1) Symmetry Force Constants and Potential Energy Distribution of D_{5h} BiF_7^{2-}

		calcd freq, cm^{-1}	symmetry force constants[a]				PED[b]
				F_{11}	F_{22}		
A_1'	ν_1	568	F_{11}	3.25			55(1) + 45(2)[d]
	ν_2	502	F_{22}	0.392	3.17		55(2) + 45(1)[e]
				F_{33}	F_{44}		
A_2''	ν_3	576	F_{33}	3.17			97(3) + 3(4)
	ν_4	287	F_{44}	0.196	1.35		100(4)
				F_{55}	F_{66}	F_{77}	
E_1'	ν_5	527	F_{55}	2.65			99(5)
	ν_6	337	F_{66}	0.893	2.92		61(6) + 30(7) + 8(5)
	ν_7	197	F_{77}	0.169	−0.359	0.716	92(7) + 7(6)
E_1''	ν_8	255	F_{88}	0.633			100(8)
				F_{99}	$F_{10,10}$		
E_2'	ν_9	456	F_{99}	2.40			71(9) + 29(10)
	ν_{10}	387	$F_{10,10}$	0.302	1.85		75(10) + 25(9)
E_2''	ν_{11}	45i[c]	$F_{11,11}$	(−0.048)[c]			

[a] Stretching force constants in mdyn/Å, deformation constants in mdyn Å/rad^2, and stretch−bend interaction constants in mdyn/rad. [b] PED in percent. The symmetry coordinates are defined as (1) νsym BiF_5 eq; (2) νsym BiF_2ax; (3) νasym BiF_2; (4) νumbrella BiF_5; (5) νasym BiF_5; (6) νasym BiF_5 in-plane; (7) δsciss BiF_2; (8) δwag BiF_2; (9) δasym BiF_5 in-plane; (10) νasym BiF_5; (11) δpucker BiF_5. [c] The negative value for $F_{11,11}$ is due to the imaginary frequency which was caused by the use of numerical differentiation in the calculation. [d] Symmetric combination of S1 and S2. [e] Antisymmetric combination of S1 and S2.

Table 8. Unscaled HF/DZP/ECP (HF/1) Symmetry Force Constants and Potential Energy Distribution of D_{5h} SbF_7^{2-}

		calcd freq, cm^{-1}	symmetry force constants[a]				PED[a]
				F_{11}	F_{22}		
A_1'	ν_1	608	F_{11}	3.60			47(1) + 53(2)[b]
	ν_2	527	F_{22}	0.514	3.65		53(1) + 47(2)[c]
				F_{33}	F_{44}		
A_2''	ν_3	640	F_{33}	3.58			93(3) + 7(4)
	ν_4	345	F_{44}	0.394	1.59		100(4)
				F_{55}	F_{66}	F_{77}	
E_1'	ν_5	559	F_{55}	2.79			97(5)
	ν_6	392	F_{66}	1.17	3.33		53(6) + 37(7) + 10(5)
	ν_7	232	F_{77}	0.298	−0.388	0.902	90(7) + 10(6)
E_1''	ν_8	293	F_{88}	0.779			100(8)
				F_{99}	$F_{10,10}$		
E_2'	ν_9	501	F_{99}	2.79			87(9) + 13(10)
	ν_{10}	377	$F_{10,10}$	0.419	1.75		88(10) + 12(9)
E_2''	ν_{11}	34	$F_{11,11}$	0.025			100(11)

[a] For dimensions and the definitions of the symmetry coordinates, see footnotes of Table 7. [b] Symmetric combination of S1 and S2. [c] Antisymmetric combination of S1 and S2.

Inspection of Tables 1, 2, and 4 reveals that, for BiF_7^{2-} and SbF_7^{2-}, the unscaled calculated HF/1 and HF/5 frequencies agree reasonably well with the experimental ones and, therefore, require no scaling. Some of the deviations between observed and calculated frequencies, such as for ν_5 and ν_6 of SbF_7^{2-} in Table 2, could be due to the presence of two strongly coupled vibrations within the same symmetry species, as shown by their relatively large interaction force constants (F_{56} in Table 8). Small variations in these interaction constants can strongly affect the frequency separation between these modes and account for some of the observed frequency deviations. The extra splittings of some of the bands observed, particularly for the low-temperature spectra of BiF_7^{2-}, can be explained by the lifting of the degeneracies for the doubly degenerate E modes and either site symmetry effects or in-phase/out-of-phase coupling of more than one molecule per unit cell. In the infrared spectra of some of the BiF_7^{2-} salts, generally a very weak but sharp band was observed at about 460 cm^{-1} which had the same frequency as one of the degenerate components of the Raman active ν_9 (E_2') mode and, therefore, is tentatively assigned to this mode. Also, in the higher frequency region of the infrared spectra, frequently some weak bands at 1050 and 960 cm^{-1} could be observed which can be attributed to the combination bands ($\nu_1 + \nu_5$) (E_1') and ($\nu_5 + \nu_9$) ($E_1' + E_2'$), respectively. Overall, the very good agreement between the calculated and observed spectra leaves no doubt that BiF_7^{2-} and SbF_7^{2-} possess pentagonal bipyramidal D_{5h} structures.

Additional support for the pentagonal bipyramidal structure of SbF_7^{2-} comes from the smooth frequency trends observed for the isoelectronic IF_7, TeF_7^-, SbF_7^{2-} series (see Table 3). The frequency and, particularly, the relative Raman intensity trends observed for the symmetric equatorial and the symmetric axial stretching modes ν_1 and ν_2, respectively, which have previously been discussed already in detail for TeF_7^-,[40] are even more pronounced for SbF_7^{2-} and BiF_7^{2-}. Thus, the mixing of the symmetry coordinates of ν_1 and ν_2 increases further when going from TeF_7^- to SbF_7^{2-} and BiF_7^{2-}, as shown by the potential energy distributions (PED) given in Tables 7 and 8. The ν_1 and ν_2 modes of SbF_7^{2-} and BiF_7^{2-} have become almost equal mixes of the corresponding symmetry coordinates, with ν_1 being their symmetric and ν_2 their antisymmetric combination. This accounts for the unusually high relative Raman intensity of ν_1 and the low intensity of ν_2 in both SbF_7^{2-} and BiF_7^{2-} and eventually even leads to an identity reversal of ν_1 and ν_2 on going from BiF_7^{2-} to AsF_7^{2-} (see PED of Table 9). A similar identity reversal is also exhibited for ν_9 and ν_{10} in the E_2' block. While in IF_7 the higher frequency mode is mainly the antisymmetric, in-plane IF_5 stretching, in BiF_7^{2-}, SbF_7^{2-}, and AsF_7^{2-}, the higher E_2' frequency mode has increasingly become the antisymmetric, in-plane deformation (see Tables 7−9).

The general frequency decrease on going from IF_7 to SbF_7^{2-} in Table 3 agrees well with our expectations. With increasing formal negative charges of the ions, the (δ+)X−F(δ−) polarity of the X−F bonds increases, which increases their ionicity and weakens them. A similar bond-weakening effect is also observed on going from SbF_7^{2-} to BiF_7^{2-} (see Tables 3). That the frequency lowerings from SbF_7^{2-} to BiF_7^{2-} cannot exclusively be a mass effect is evident from the decrease in the frequencies of ν_1, in which the central atom does not move.

The symmetry force constants and potential energy distributions for BiF_7^{2-}, SbF_7^{2-}, and AsF_7^{2-} are summarized in Tables 7−9. Since for some of the infrared active modes of BiF_7^{2-} and SbF_7^{2-} and for all modes of AsF_7^{2-} no experimental data were available, the unscaled HF/DZP/ECP (HF/1) frequencies

Table 9. Unscaled HF/DZP/ECP (HF/1) Frequencies Symmetry Force Constants and Potential Energy Distribution of D_{5h} AsF_7^{2-}

		calcd freq, cm^{-1}	symmetry force constants[a]				PED[a]
			F_{11}	F_{22}			
A_1'	ν_1	656	F_{11}	3.89			65(2) +35(1)[b]
	ν_2	549	F_{22}	0.693	4.31		65(1) +35(2)[c]
				F_{33}	F_{44}		
A_2''	ν_3	742	F_{33}	4.23			83(3) +17(4)
	ν_4	430	F_{44}	0.591	1.93		100(4)
				F_{55}	F_{66}	F_{77}	
E_1'	ν_5	567	F_{55}	2.69			98(5) +2(7)
	ν_6	470	F_{66}	1.75	4.21		37(7) +31(5) +31(6)
	ν_7	294	F_{77}	0.477	−0.387	1.18	85(7) +13(6) +2(5)
E_1''	ν_8	357	F_{88}	0.994			100(8)
				F_{99}	$F_{10,10}$		
E_2'	ν_9	600	F_{99}	3.67			96(9) +4(10)
	ν_{10}	291	$F_{10,10}$	0.610	1.08		95(10) +5(9)
E_2''	ν_{11}	91	$F_{11,11}$	0.159			100(11)

[a] For dimensions and definitions of the symmetry coordinates, see footnotes of Table 7. [b] Symmetric combination of S1 and S2. [c] Antisymmetric combination of S1 and S2.

Table 10. Internal Stretching Force Constants[a] (mdyn/Å) of the Isoelectronic Series XeF_7^+, IF_7, TeF_7^-, and SbF_7^{2-} and of the Pnicogen(V) Heptafluoride Dianion Series (b)

	series a				series b		
	XeF_7^+	IF_7	TeF_7^-	SbF_7^{2-}	BiF_7^{2-}	SbF_7^{2-}	AsF_7^{2-}
$f_{D(ax)}$	5.046	5.005	4.415	3.61	3.21	3.61	4.27
f_{DD}	0.088	0.058	0.045	0.04	0.04	0.04	0.04
$f_{d(eq)}$	4.144	3.947	3.091	2.534	2.434	2.534	2.286
$f_{dd(adjac)}$	0.117	0.326	0.538	0.500	0.363	0.500	0.761
$f_{dd'(oppos)}$	0.034	0.047	-0.003	0.033	0.005	0.033	0.041

[a] It should be noted that the values for XeF_7^+, IF_7, and TeF_7^- from refs 39 and 40 are scaled by factors of 0.8636 and 0.8649, respectively, whereas the SbF_7^{2-} and AsF_7^{2-} values are unscaled values from this study. The SbF_7^{2-} values were not scaled in view of the very close agreement between experimentally observed and calculated frequencies (see Table 3), which eliminated the need for using a scaling factor.

and force fields were used for all three anions to allow a better comparison. Most of the implications of this normal coordinate analysis have already been discussed and do not need to be reiterated, except for emphasizing that, when comparing the results from this study with the previous analyses of IF_7[39] and TeF_7^-,[40] attention must be paid to the different identities, i.e., reversal of assignments, for ν_1 and ν_2 and ν_9 and ν_{10}.

Of the internal force constants, only the stretching force constants are fully determined[39] and are given in Table 10. For all compounds, the axial stretching force constants are significantly larger than the equatorial ones. This finding is in excellent agreement with the bonding scheme previously proposed[39] for IF_7. It involves a planar, delocalized p_{xy} hybrid orbital of the central atom for the formation of five equatorial, semi-ionic, 6-center, 10-electron bonds and an sp_z hybrid for the formation of two mainly covalent axial bonds. Depending on the degree of congestion in the equatorial plane, the equatorial fluorine ligands can undergo varying degrees of fast dynamic puckering which, together with a slower intramolecular equatorial−axial ligand exchange, account for the fluxionality of these molecules.[39] As expected, increasing formal negative charges increase the $(\delta+)X-F(\delta-)$ polarity and, hence, the ionic character of the X−F bonds and explain the observed bond-weakening encountered on going from XeF_7^+ to SbF_7^{2-}. It is interesting to note the strong influence the increasing formal negative charges have on f_{dd}, the coupling constant between adjacent equatorial X−F bonds. With increasing ionicity of the X−F bonds, the coupling between adjacent bonds strongly increases, while the coupling between opposite equatorial bonds (f_{dd}') remains negligible. Within the BiF_7^{2-}, SbF_7^{2-}, and AsF_7^{2-} series, where the number of formal negative charges is constant but the size and the mass of the central atom decrease, very interestingly the force constant of the more covalent axial bonds increases from BiF_7^{2-} to AsF_7^{2-} while at the same time that of the more ionic equatorial bonds has its lowest value for AsF_7^{2-}. This effect might be explained by the increasing tendency of the XF_7^{2-} species to lose with decreasing size of the central atom one fluoride ion with formation of a more covalent XF_6^- anion. Similar to the XeF_7^+, IF_7, TeF_7^-, and SbF_7^{2-} series, there is again a very strong increase in f_{dd}, the coupling constant of the adjacent equatorial fluorine ligands, despite a decrease in the f_d values.

Although explicit values for the internal deformation constants cannot be given without the assumption of certain constraints, several general conclusions concerning the relative magnitudes of the in-plane (f_α) and out-of-plane (f_β) deformation constants and their trends can be reached from an inspection of their corresponding symmetry force constants in Tables 7−9 and ref 39 and 40 (it should be noted that Table 1 of ref 40 contains an error in the approximate mode descriptions for ν_6 and ν_7, which have been transposed). As expected, the equatorial in-plane deformation constants, f_α, increase with increasing stiffening of the X−F bonds on going from SbF_7^{2-} to XeF_7^+, which to a lesser extent is also the case for the out-of-plane deformation constant, f_β. Similarly, the increases in both f_α and f_β on going from BiF_7^{2-} to AsF_7^{2-} are expected on the basis of the shortening of the bonds. This strong increase in the deformation force constants, coupled with a simultaneous slight decrease of the equatorial stretching force constant, accounts for the increased coupling between stretching and deformation modes and some of the observed identity reversals encountered on going from BiF_7^{2-} to AsF_7^{2-}.

Conclusions

In view of the long known existence and widespread use of the pnicogen(V) hexafluoride anions and the easy syntheses and great stabilities of the previously unknown pnicogen(V) heptafluoride dianions, it is truly amazing that no previous reports on the existence of these dianions could be found in the literature. This appears to be another example for general preconceptions about what may and may not exist, having stopped chemists from openmindedly searching for certain simple species. It is this kind of dogmatic thinking (in our case, the magic stability attributed to the octahedral "sp^3d^2" type electronic configurations) which had delayed for a long time the discovery of noble gas compounds.[49]

Acknowledgment. This article is dedicated to Prof. George A. Olah on the occasion of his 70th birthday. The authors thank Drs. S. Rodgers, P. Carick, and G. Olah for their active support. The work at the Air Force Research Laboratory was financially supported by the Propulsion Directorate and Office of Scientific Research of the Air Force, that at USC by the National Science Foundation, and that at PNNL by the Department of Energy. G.W.D. gratefully acknowledges the National Research Council for a postdoctoral fellowship at AFRL.

JA9805728

(43) Bougon, R.; Charpin, P.; Christe, K. O.; Isabey, J.; Lance, M.; Nierlich, M.; Vigner, J.; Wilson, W. W. *Inorg. Chem.* **1988**, *27*, 1389.
(44) Christe, K. O.; Wilson, R. D.; Schack, C. J. *Inorg. Chem.* **1977**, *16*, 937.
(45) Siebert, H. *Anwendungen der Schwingungsspektroskopie in der Anorganischen Chemie*; Springer-Verlag: Berlin, 1966.
(46) Hebecker, C. *Z. Anorg. Allg. Chem.* **1971**, *384*, 12.
(47) Zhang, X.; Christe, K. O. Unpublished data for $ClF_4^+SbF_6^-$.
(48) Gafner, G.; Kruger, G. J. *Acta Crystallogr., Sect. B* **1974**, *B30*, 250.
(49) Bartlett, N. *Proc. Chem. Soc.* **1962**, 218.